archives
of thermodynamics
Vol. **42**(2021), No. 3, 141–158
DOI: 10.24425/ather.2021.138113

Diffusive–inertial droplet separation model from two-phase flow

JAROSŁAW MIKIELEWICZ
OKTAWIA DOLNA*
ROMAN KWIDZIŃSKI

Institute of Fluid Flow Machinery, Polish Academy of Sciences,
Fiszera 14, 80-231 Gdansk, Poland

Abstract This paper concerns analytical considerations on a complex phenomenon which is diffusive-inertial droplet separation from the two-phase vapour-liquid flow which occurs in many devices in the power industry (e.g. heat pumps, steam turbines, organic Rankine cycles, etc.). The new mathematical model is mostly devoted to the analysis of the mechanisms of diffusion and inertia influencing the distance at which a droplet separates from the two-phase flow and falls on a channel wall. The analytical model was validated based on experimental data. The results obtained through the analytical computations stay in a satisfactory agreement with available literature data.

Keywords: Two-phase flow; Diffusive-inertial droplet separation; Stopping distance

Nomenclature

c	–	concentration of droplets, kg/m^3
D	–	droplet diameter, m
D_m	–	droplet average diameter, m
$f(D_c)$	–	coefficient (Eq. (20))
g	–	gravitational acceleration, m^2/s
$g(y^+)$	–	distribution function of the separating droplets mass flux along the y^+ direction
K	–	parameter, 1/s

*Corresponding Author. Email: odolna@imp.gda.pl

k	–	mass transfer coefficient
L	–	channel length, m
l	–	mixing path, m
m	–	droplet mass, kg
$\dot{m}$	–	mass velocity, kg/(s m^2)
$p(D)$	–	probability density of droplets diameter distribution
R	–	radius of curvature of the channel, m
Re	–	Reynolds number
s	–	stopping distance or path of a droplet, m
s_M	–	stopping distance with Magnus lift force included, m
t	–	time, s
u_d, v_d	–	horizontal and vertical components of the velocity of droplets in a horizontal channel or component of the velocity which is parallel and perpendicular to the pipes' wall, respectively, in a case of a slope channel, m/s
u_l	–	liquid velocity, m/s
u_t, v_t	–	horizontal and vertical components of a droplet tangential velocity, m/s
u_ν	–	vapour velocity, m/s
v	–	continuous phase velocity, m/s
v_0	–	shear velocity, m/s
z	–	distance at which given mass of droplets is separated, m
y	–	distance from the wall, m
y^+	–	dimensionless wall normal distance

Greek symbols

ρ	–	density, kg/m^3
μ	–	dynamic viscosity, Pa s
ν	–	kinematic viscosity, m^2/s
δ	–	thickness of the boundary layer, m
κ	–	turbulence constant in the Prandtl mixing model
ε	–	diffusivity of droplets
τ	–	shear stresses, Pa
τ^+	–	dimensionless relaxation time
ϕ	–	variable

Subscripts

c	–	critical
d	–	droplet
ih	–	relates to the mixing path
il	–	inertial laminar
l	–	liquid
m	–	when this subscript is accompanied by d it relates to the mean diameter of droplets
ν	–	vapour
$+$	–	relates to dimensionless quantities
0	–	relates to the velocity of the continuous phase

1 Introduction

Separation of droplets from the two-phase flow of wet vapour is an important issue related to the steam dryers in refrigerating and air-conditioning systems. This phenomenon is also present in steam turbines as well as in the organic Rankine cycles (ORCs). During vapour generation in boilers and heat exchangers, the flow-boiling process takes place which is associated with the occurrence of a so-called boiling crisis (dryout). The boiling crisis starts up when a liquid film dries out on the heated channel wall [1,2] Further heat supply to the channel wall cause the annular flow regime to occur with the vapour presence on the channel wall and drying droplets in the two-phase flow core. Effective cooling of hot gases involves injecting cold water into them which is atomised and the mist flow is being formed. In all these processes, the droplets are being separated from the flow as they deposit on the channel wall.

There are several mechanisms causing the motion of droplets in the continuous phase. This motion can be caused by molecular or turbulent diffusion of the vapour. The gaseous phase velocity field and its gradients [3] are of a significant meaning as they may cause rotational movement of droplets and the associated droplet separating forces. Moving droplets have their inertia which depends on the mass of droplets. The droplets' inertia causes the velocity field and the trajectories of droplets not to coincide with the velocity field of the gaseous phase. During motion, the droplets coalesce or break down. This causes continuous changes in the statistical distribution of droplets in the flow. The process of droplet separation from the two-phase flow is complex and has not yet been fully explained. The developed to date models and dependencies describing this process are of a fragmented character and concern only a small range of the two-phase flow with droplet separation.

In this paper, the authors proposed their own model of the diffusive-inertial separation of droplets. In engineering calculations, the influence of the boundary layer, in which droplets move and rotate, is usually neglected. In the flow within the boundary layer, Magnus and Saffman force act on droplets [4, 5], causing a change in both their trajectory and distance at which droplet separates on the channel wall [6].

The paper contains a novel model which is not available in the literature. Regarding the literature in the field of the current paper's subject, there are many works on the aerosol deposition issue. In the paper by Pourhashem *et al.* [7], investigations on the deposition of the aerosol com-

ing from e-cigarette was considered. It was confirmed that deposition of the contained ingredients occurs due to diffusive vapour transport. Worth Longest *et al.* [8] in their work raise the problem of the inertia effect on submicron particles separation as the inertia is being mostly neglected in the case of the 0.2 μm particles. The authors have worked on the evaluation of the conditions at which the inertia effects become meaningful when compared to diffusional effects. Authors of [9] strongly emphasise the influence of a centrifugal acceleration and velocity on separation.

2 Novel diffusive-inertial liquid-vapour separation model

Let us assume that the statistical distribution of droplets in two-phase flow is known. Information on the statistical distribution of droplets in the mist flow in the channel can be found in [2, 10] Droplets can be divided into fractions according to their size. Within the framework of the research presented herein, the droplets were divided into two fractions. The first fraction covers small droplets some of which can deposit on the channel wall according to the conventional mechanism of turbulent diffusion of the gaseous phase. The second fraction includes larger droplets which can settle on the wall according to the turbulent-inertial mechanism.

The droplets from the first fraction are small enough (order of magnitude $\sim 10^{-6}$) that their inertia does not affect their movement in the gas velocity field. They keep up with the turbulent fluctuations of this velocity field. Such a mass transfer process is commonly known [11, 12].

The further part of the paper deals with the diffusive-inertial mechanism of separation of the second droplet fraction. For these droplets, it is necessary to consider their inertia during motion. The droplets lag behind the turbulent motion of groups of molecules and, therefore, they cannot get to the wall through the laminar sublayer within which molecules exhibit only the molecular motion. These droplets can reach the channel wall as a result solely of their inertial motion, stemming from the impulse they received in the turbulent sublayer of the flow.

It is well known that turbulent vortices get bigger, the farther away they are from the channel wall. This results directly from Prandtl's turbulence model, in which the scale of turbulent vortexes can be determined on the basis of the so-called mixing path. The scale of inertial motion of a droplet can be defined using the stopping distance of this droplet after receiving

the impulse. If a vortex is large enough, far away from the channel wall, the droplet can keep up with the motion within such a vortex. However, if vortices are too small compared to the droplet's stopping distance, the droplet ignores them and either moves to a distance equal to the stopping distance or continues to move in accordance with the direction of the gravitational and the centrifugal resultant forces.

The inertial-turbulent model of separation of droplets, presented below, is described in a quantitative manner. The assumptions of this model can be summarised as follows:

1. If the path of the turbulent mixing of the gaseous phase is longer than the droplet's stopping distance, the droplet is subjected to the diffusion of the turbulent gaseous phase.

2. If the path of the turbulent mixing of the gaseous phase is shorter than the droplet's stopping distance, the droplet is subjected to the inertial diffusion. Inertial diffusion is analogous to turbulent diffusion and depends on the stopping distance of droplets, similarly as turbulent diffusion depends on the Prantl's mixing path.

3. Droplets featuring large inertia, and which are also affected by the Magnus force, can get through the laminar sublayer, where high velocity gradients exist.

The development of the proposed droplet separation model required carrying out an analysis of the movement of a single droplet.

2.1 Stopping distance of a droplet during its inertial motion

In the case when only the drag and Magnus forces are taken into consideration, bearing in mind that the flow trajectory is relatively flat, the droplet motion equations for horizontal and vertical velocity components (u_d and v_d, respectively) can be written in the following form:

$$\rho_l \frac{\pi}{6} D^3 \frac{du_d}{dt} = -3\pi\mu_\nu D\left(u_\nu - u_d\right), \tag{1}$$

$$\rho_l \frac{\pi}{6} D^3 \frac{dv_d}{dt} = -3\pi\mu_\nu D v_d + \rho_\nu \frac{\pi}{8} D^3 (u_v - u_d)\frac{du_v}{dy}. \tag{2}$$

Due to the small size of the droplet, it was assumed in this equation that the flow around it is laminar and its path is rather flat [3]. On the right side of Eq. (1), the first term relates to Stokes drag force.

In Eq. (2), on the right side, there is drag force and Magnus force as α (see Fig. 1) is relatively small. The Eqs. (1) and (2) can be rewritten in the following form:

$$\frac{du_d}{dt} = -K\left(u_\nu - u_d\right), \tag{3}$$

$$\frac{dv_d}{dt} = -Kv_d + \frac{3}{4}\frac{\rho_\nu}{\rho_l}(u_v - u_d)\frac{du_v}{dy}, \tag{4}$$

where $K = \dfrac{18\mu_\nu}{\rho_l D^2}$.

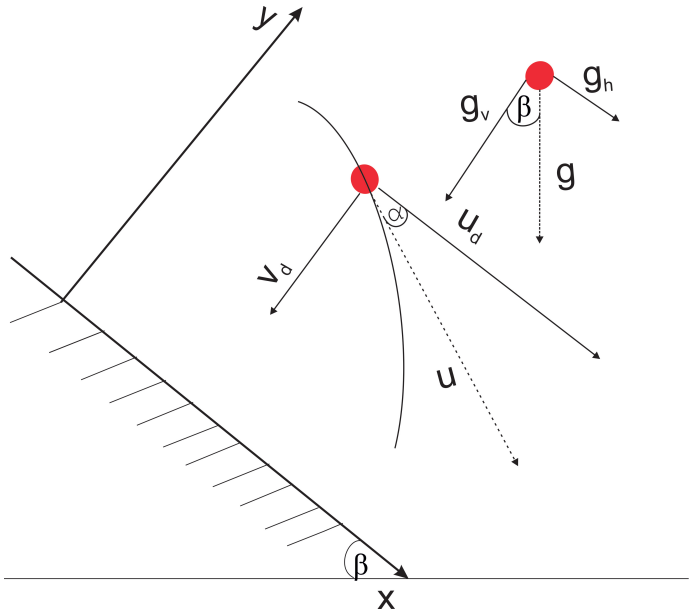

Figure 1: Pictorial view of the velocity vector and the gravity acting on a droplet.

By determining the velocity difference $(u_v - u_d)$ from Eq. (3) and inserting it into (4), and also assuming that $\dfrac{du_d}{dy} \approx \dfrac{du_\nu}{dy}$, one obtains

$$\frac{dv_d}{dt} = -v_d\left[K + \frac{3}{4K}\frac{\rho_\nu}{\rho_l}\left(\frac{du_\nu}{dy}\right)^2\right]. \tag{5}$$

The above equation can be integrated twice with the following initial conditions: $t = 0$, $v = v_0$, and $s = 0$. In result, for $t \to \infty$ one obtains the so-called stopping distance taking into account the Magnus force

$$s_M = \frac{v_0}{K + \frac{1}{K}\frac{3}{4}\frac{\rho_\nu}{\rho_l}\left(\frac{du_\nu}{dy}\right)^2}. \tag{6}$$

If the Magnus force is neglected, the relation (6), due to small velocity gradients, simplifies to

$$s = \frac{v_o}{K}. \tag{7}$$

Noting that in the laminar sublayer

$$\frac{du_\nu}{dy} = \frac{\tau}{\mu_\nu} = \frac{v_o^2}{\nu_\nu} \tag{8}$$

relationships (6) and (7) can be presented in the following dimensionless form:

$$s^+ = \frac{sv_o}{\nu_\nu} = \frac{1}{18}\frac{\rho_l}{\rho_\nu}\left(D^+\right)^2, \tag{9}$$

$$s_M^+ = \frac{s_M v_o}{\nu_\nu} = \frac{s^+}{1 + \frac{1}{18}\frac{\rho_l}{\rho_\nu}\left(D^+\right)^2}, \tag{10}$$

where $D^+ = \dfrac{Dv_o}{\nu_\nu}$ and $v_o = \sqrt{\dfrac{\tau}{\rho_\nu}}$ is the shear velocity.

2.2 Limit of the diffusive–inertial layer

The lower limit of the layer, in which the droplets diffusion is related to their inertia, can be assumed, for the sake of simplicity, as the distance from the wall ($\delta_{il}^+ = 5$) equal to the stopping distance s^+. The limit $\delta_{il}^+ = 5$ will also be adopted for droplets of diameter slightly greater than the critical (D_c) since such droplets are able to get through the laminar sublayer with the aid of Magnus force acting in this sublayer – as explained in previous considerations.

Summing up, in the analysed model of droplets separation from the mist flow, one can make an assumption that the lower limit of the inertial layer is defined as

$$\delta_{il}^+ = \begin{cases} s^+ & \text{for } \; s^+ \geq 5, \\ 5 & \text{for } \; s^+ < 5. \end{cases} \tag{11}$$

The upper limit of the inertial layer results from the second assumption of the model that mixing path is equal to stopping path which can be expressed quantitatively as follows:

$$l_{il}^{+} = s^{+}. \tag{12}$$

At the boundary layer upper limit, the mixing path can be calculated from

$$l_{il}^{+} = \kappa \delta_{ih}^{+}, \tag{13}$$

where $\kappa = 0.58{-}0.4$ is the turbulence constant in the Prandtls' model.

Now, one can obtain the upper limit of the inertial sublayer from Eq. (12)

$$\delta_{ih}^{+} = \frac{s^{+}}{\kappa} = \frac{1}{18\kappa} \frac{\rho_l}{\rho_\nu} \left(D^{+}\right)^2. \tag{14}$$

At a distance from the wall greater than the upper limit of the inertial layer there are vortexes larger than the stopping distance, thereby the droplets can keep up with their movement.

2.3 Diffusivity of droplets in the inertial and turbulent layer

Within the inertial zone, when $\delta_{il}^{+} < y^{+} < \delta_{ih}^{+}$, the diffusion of droplets moving towards the wall can be determined analogously to the diffusion of a turbulent motion (according to Prandtl's model. Therefore,

$$\varepsilon_d = s^2 \frac{du_\nu}{dy}. \tag{15}$$

The velocity gradient can be determined from the shear stress in the turbulent motion using the following relation:

$$\tau = \rho_\nu \varepsilon_\nu \frac{du_\nu}{dy} = \rho_\nu l^2 \left(\frac{du_\nu}{dy}\right)^2. \tag{16}$$

Noting that $v_o = \sqrt{\dfrac{\tau}{\rho_\nu}}$, one gets from (16)

$$\frac{du_\nu}{dy} = \frac{v_0}{l}. \tag{17}$$

Substituting (15) into (17), one can obtain the diffusivity of droplets in the dimensionless form,

$$\varepsilon_d^+ = \frac{\varepsilon_d}{\nu_\nu} = \frac{1}{\kappa}\frac{(s^+)^2}{y^+} = \frac{1}{324\kappa}\left(\frac{\rho_l}{\rho_\nu}\right)^2 \frac{(D^+)^4}{y^+}. \tag{18}$$

Within the turbulent layer, the diffusion of droplets is governed by the medium's turbulence, that is

$$\varepsilon_\nu^+ = \frac{\varepsilon_\nu}{\nu_\nu} = \varepsilon_d^+ = \kappa y^+. \tag{19}$$

2.4 Statistical distribution of droplets in the mist flow

In the subject literature, various experimental correlations that describe the statistical distributions of droplets in the mist flow can be found, e.g. [2, 10]. Typically, these distributions have the shape of a bell curve with the maximum value shifted towards lower diameters of droplets. Therefore the most probable diameter of droplets is about half the average diameter. The statistical distribution of droplets, designated as $p(D)$, depends on the droplet average diameter D_m. The average diameter of droplets can be calculated using experimental formulas [10], depending on the way the droplets are generated. If the probability density $p(D)$ for the occurrence number of droplets of a given diameter is known, one can estimate the mass ratio of the droplets which diameter exceeds a certain given value to the mass of all droplets. For droplets with diameter greater than critical, this ratio is evaluated from:

$$f(D_c) = \frac{\int_{D_c}^{\infty} D^3 p(D)\,\mathrm{d}D}{\int_0^{\infty} D^3 p(D)\,\mathrm{d}D}. \tag{20}$$

Coefficient $f(D_c)$ allows to determine the fraction of droplets that are subjected to the turbulent-inertial separation mechanism.

In [10] the probability distribution is given in the following form:

$$p(D) = 4\left(\frac{D}{D_m}\right)^2 e^{-2\frac{D}{D_m}}. \tag{21}$$

2.5 Mass flux of droplets depositing on the channel wall

The mass velocity of droplets with a diameter of $D \pm dD$ which deposit on the wall in the diffusive-inertial manner, is expressed through

$$d\dot{m} = \varepsilon_d \frac{\partial^2 c(D)}{\partial D \partial y} dD, \tag{22}$$

which results from the mass transfer equation, $\dot{m}(D) = \varepsilon_d \dfrac{dc}{dy}$, where ε_d denotes the diffusivity of the droplets with a diameter D, c is the concentration of such droplets and y is the distance from the wall.

The ratio of the mass of the droplets with a diameter of $D \pm \mathrm{d}D$ to the mass of all droplets can be written as follows:

$$\frac{d\dot{m}(D)}{\dot{m}} = \frac{D^3 p(D) dD}{\int\limits_0^\infty D^3 p(D) \mathrm{d}D} = \phi(D) dD = \frac{dc(D)}{c(D)}\,, \tag{23}$$

where $c = \dfrac{m_l}{\dfrac{m_l}{\rho_l} + \dfrac{m_v}{\rho_v}}$.

It follows from (23) that

$$\frac{\partial^2 c(D)}{\partial D \partial y} = \phi(D) \frac{dc(D)}{dy}\,. \tag{24}$$

Combining (22) and (24), one gets

$$d\dot{m}(D) = \varepsilon_d \phi(D) \frac{dc(D)}{dy} dD\,. \tag{25}$$

The relation (25) can be written in the dimensionless form as

$$d\dot{m}^+ \left(D^+\right) = \varepsilon_d^+ \phi^+(D^+) \frac{dc(D^+)}{dy^+} dD^+ \tag{26}$$

with $\varepsilon_d^+ = \dfrac{\varepsilon_d}{\nu_\nu}$, $\phi^+ = \dfrac{\nu_\nu}{v_o}\phi$, $c^+ = \dfrac{c}{\rho_\nu}$, $y^+ = \dfrac{y v_o}{\nu_\nu}$, $\dot{m}^+ = \dfrac{\dot{m}}{v_0 \rho_\nu}$, $D^+ = D\dfrac{v_0}{\nu_\nu}$, where $\dot{m}$ is a mass velocity.

Equation (26) can be integrated within the limits of the inertial sublayer and then within the limits of the turbulent sublayer (bounded by the

thickness of the boundary layer or by the channel radius) with the following boundary conditions:

$$c^+ = \begin{cases} 0 & \text{for} \quad y^+ = \delta_{ih}^+ , \\ c_\infty & \text{for} \quad y^+ = \delta^+ , \end{cases}$$

where c_∞ represents concentration of droplets far from the wall. Assuming that $d\dot{m}$ and $d\dot{m}_w g(y^+)$ are equal to each other, one then obtains the mass flux of droplets depositing on the channel wall, namely

$$\frac{\dot{m}_w}{v_o \rho_\nu} = \int\limits_{D_c^+}^{\infty} \frac{\phi\left(D^+\right) \mathrm{d}D^+}{\int\limits_{\delta_{ih}^+}^{\delta^+} \frac{g(y^+)\mathrm{d}y^+}{\varepsilon_\nu(y^+)} + \int\limits_{\delta_{il}^+}^{\delta_{ih}^+} \frac{g(y^+)\mathrm{d}y^+}{\varepsilon_d(y^+, D^+)}} , \tag{27}$$

where $g(y^+)$ is the distribution function for the mass flux of the droplets along the y^+ coordinate (y^+ – dimensionless wall normal distance). The integrals appearing in Eq. (27) can be calculated analytically for simple cases, such as a plate or a pipe, which is shown in the next section. To simplify these calculations, it can be assumed that the denominator of (27) is evaluated for the average diameter of droplets (D_m). The simplified equation is following

$$\frac{\dot{m}_w}{v_o \rho_\nu} = \frac{f(D_m^+)}{\int\limits_{\delta_{ih}^+}^{\delta^+} \frac{g\left(y^+\right) \mathrm{d}y^+}{\varepsilon_\nu(y^+)} + \int\limits_{\delta_{il}^+}^{\delta_{ih}^+} \frac{g\left(y^+\right) \mathrm{d}y^+}{\varepsilon_d(y^+, D_m^+)}} , \tag{28}$$

As shown by the calculations for simple cases, the diffusion resistance of the inertial layer is much lower than the resistance of the turbulent diffusion. Therefore in approximate calculations, the resistance of the inertial layer can be neglected. In such a case, the simplified relation (28) can be simplified even further

$$\frac{\dot{m}_w}{v_o \rho_\nu} = \frac{f(D_m^+)}{\int\limits_{\delta_{ih}^+}^{\delta^+} \frac{g\left(y^+\right) \mathrm{d}y^+}{\varepsilon_\nu(y^+)}} . \tag{29}$$

Integrals in Eqs. (20) and (27) should be calculated within the limits from D_c^+ to the largest droplets present in the flow. The maximum droplet diameter can be estimated based on the critical Weber number [10]. However,

trial calculations prove that if the upper integration limit is left infinite then the calculation error is small.

3 Solutions for a plate and a pipe

In the case of a plate, the shear stresses (τ) and the separating droplet mass velocity $\dot{m}_w$ are constant along the y coordinate. Therefore, the shear velocity (v_0) and the density distribution of the flux, denoted by $g(y^+)$, are constant too. Taking into account this fact, and employing dependencies (18) and (19) in Eq. (27), one gets the following dependency for the plate:

$$\frac{\dot{m}_w}{v_o \rho_\nu} = c_\infty^+ \int_{D_{c^+}}^{\infty} \frac{\phi(D^+)\,\mathrm{d}D^+}{\dfrac{1}{\kappa}\ln\dfrac{\delta^+}{\delta_{ih}^+} + \dfrac{162\kappa}{(D^+)^4}\left(\dfrac{\rho_f}{\rho_l}\right)^2\left(\delta_{ih}^{+2} - \delta_{il}^{+2}\right)}\,. \tag{30}$$

Assuming, in turn, that the calculations are done for an average-sized droplet, this dependency can be simplified to the following form:

$$\frac{\dot{m}_w}{v_o \rho_\nu} = c_\infty^+ f \frac{1}{\dfrac{1}{\kappa}\ln\dfrac{\delta^+}{\delta_{ih}^+} + \dfrac{162\kappa}{(D^+)^4}\left(\dfrac{\rho_f}{\rho_l}\right)^2\left(\delta_{ih}^{+2} - \delta_{il}^{+2}\right)}\,, \tag{31}$$

where f is the distribution of droplets.

For a pipe, the shear stresses change linearly along the y coordinate. These stresses can be expressed as follows:

$$\tau = \tau_w \frac{r}{R} = \tau_w \left(1 - \frac{y^+}{R^+}\right), \tag{32}$$

where τ_w is the wall shear stress. When the shear stresses change, the dynamic velocity and the stopping distance also change. Thus

$$v_0 = \sqrt{\frac{\tau}{\rho_l}} = v_w \sqrt{1 - \frac{y^+}{R^+}} \tag{33}$$

and inserting (33) to (7), one obtains the stopping distance in the following form:

$$s^+ = s_w^+ \sqrt{1 - \frac{y^+}{R^+}}. \tag{34}$$

By using the dependency (34) in formula (18), one gets the diffusivity of droplets in the inertial layer

$$\varepsilon_d^+ = \frac{\varepsilon_d}{\nu_\nu} = \frac{1}{\kappa}\frac{\left(s^+\right)^2}{y^+} = \frac{1-\dfrac{y^+}{R^+}}{\kappa}\frac{\left(s_w^+\right)^2}{y^+}\,. \tag{35}$$

Compared to the plate, for the pipe, the velocity gradient that occurs in the turbulent diffusivity of the medium (ε_ν) changes. Let us determine this gradient. In the turbulent zone, the shear stresses are described by the dependency (16). By inserting this dependency to the formula that defines stresses (32), one obtains the following relation:

$$\frac{du_\nu}{dy} = \frac{\sqrt{1-\dfrac{y^+}{R^+}}}{\kappa}\frac{1}{y^+}\frac{v_0}{l}\,. \tag{36}$$

By inserting (36) to (19), one gets the following dependency:

$$\varepsilon_\nu^+ = \kappa y^+\sqrt{1-\frac{y^+}{R^+}}\,. \tag{37}$$

For the pipe, compared to the plate, the limit of the inertial layer changes – due to changes in the stopping distance $\left(s^+\right)$ which is expressed by dependency (34). By comparing the mixing path with the stopping distance (43), one obtains a quadratic equation with the δ_{ih} variable. The solution of this equation is the following:

$$\delta_{ih}^+ = \frac{\left(s_w^+\right)^2}{\kappa^2}\left(-\frac{1}{2R^+}+\frac{1}{2}\sqrt{\frac{1}{\left(R^+\right)^2}+\frac{4\kappa^2}{\left(s_w^+\right)^2}}\right). \tag{38}$$

For large values of R^+, dependency (38) is the same as dependency (14) – in other words, it is the same as for the plate. By using dependencies (35) and (38) and assuming, by analogy with the stresses, that the density distribution of droplets that separate themselves is expressed in the form

$$\dot{m} = \dot{m}_w\left(1-\frac{y^+}{R^+}\right) = \dot{m}_w g\left(y^+\right), \tag{39}$$

one can calculate, using (30), the fluid mass flux of the droplets that separate themselves in the pipe using the following dependency:

$$\frac{\dot{m}_w}{v_0\rho_\nu} = c_\infty^+ \int_{D_c^+}^{\infty} \frac{\phi(D^+)\,\mathrm{d}D^+}{\frac{2}{\kappa}\mathrm{arcth}\sqrt{1-\frac{\delta_{ih}^+}{R^+}} - 2\sqrt{1-\frac{\delta_{ih}^+}{R^+}} + \frac{162\kappa}{(D^+)^4}\left(\frac{\rho_\nu}{\rho_l}\right)^2\left(\delta_{ih}^{+2}-\delta_{il}^{+2}\right)}. \quad (40)$$

Assuming that the mass transfer is dependent upon the average droplet size, dependency (40) can be simplified to the given form

$$\frac{\dot{m}_w}{v_0\rho_\nu} = c_\infty^+ f \frac{1}{\frac{2}{\kappa}\mathrm{arcth}\sqrt{1-\frac{\delta_{ih}^+}{R^+}} - 2\sqrt{1-\frac{\delta_{ih}^+}{R^+}} + \frac{162\kappa}{(D^+)^4}\left(\frac{\rho_\nu}{\rho_l}\right)^2\left(\delta_{ih}^{+2}-\delta_{il}^{+2}\right)}. \quad (41)$$

The above mass transfer dependencies can be written in a more conventional manner, as follows:

$$\frac{\dot{m}_w}{v_0\rho_\nu} = c_\infty^+ k^+, \quad (42)$$

where k^+ is a dimensionless mass transfer coefficient. The value of this coefficient can be easily determined using the given dependencies.

In general, if diffusion is supported by body forces, the mass flux of the separated droplets for the one-dimensional case can be expressed by the following equation:

$$\dot{m}_w = -\varepsilon_d \frac{dc}{dr} + v_m c\,, \quad (43)$$

where $v_m$is the velocity of droplets which results from the body forces.

The velocity of the sedimentation of droplets due to gravitational force and centrifugal force results from the balance between the drag force and the body forces. In the case of the Stokes force, one obtains

$$v_m = \frac{\rho_d g D_d^2}{18\mu_\nu} + \frac{\rho_d v_t^2 D_d^2}{18\mu_\nu R} = \frac{\rho_d\left(\frac{v_t^2}{R}+g\right)D_d^2}{18\mu_\nu}. \quad (44)$$

The sedimentation of droplets on a dry wall is twice as intense as their settlement on a wet wall or on a liquid layer. This is due to bouncing the droplets off the liquid surface or entrainment.

3.1 Sample calculation results

The results of the proposed model were tested for the case of vapour-liquid flow in a straight vertical pipe. Using (41), the mass velocity of separated ammonia and water droplets was calculated and compared with experiments.

Several experiments concerning droplet or solid particle separation in vertical flows have been published. Downward flow of water droplets in an air stream was investigated in [13]. Similar considerations were reported in [14] for ragweed pollen and [11] for olive oil droplets. Deposition in vertical turbulent flow was also studied in [15], for iron and aluminium powder, as well as in [16, 17] for uranine and methylene blue dyes. All these results have been summarized in [18] as a dependence between the mass transfer coefficient (k^+) from (42) and dimensionless relaxation time defined as

$$\tau^+ = \frac{D^2 \rho_\nu \rho_d \nu_0^2}{18 \mu_\nu^2} \,. \tag{45}$$

Following this approach, the solution of (41) is also presented in terms of these two parameters.

It was assumed in the calculations that the droplets had formed by condensation in a flow of ammonia or water vapour in a straight pipe of 0.1 m internal diameter (ID). The droplet concentration was set to $c = 10$ kg/m^3 although the results presented below are independent of it. Average vapour velocity u_ν was assumed equal to 10 m/s or 20 m/s. It was also assumed that both phases are in thermal equilibrium under saturation conditions. Two temperature values were considered for each fluid: −30°C and 0°C for ammonia or 100°C and 200°C for water. The range of droplet diameters for which Eq. (41) is valid is determined by the model assumptions concerning the inertial sublayer limits. Namely, the minimal diameter follows from assumption $\delta_{il}^+ = 5$ (11), while the largest one from the condition $\delta_{il}^+ < \delta_{ih}^+$.

The calculation results are shown in Fig. 2. The model solution is in good agreement with the experimental data for both fluids considered. In all cases, the solution starts from $\tau^+ = 5$ and finishes at $k^+ \approx 0.6$. Limiting physical droplet diameters are mentioned in the caption of Fig. 2. Regarding flow velocity, higher mass transfer coefficients are predicted for lower velocities. This however translates to higher separated mass flux for higher flow velocity (due to the fact that the dynamic velocity rises with flow velocity, equalling for example here in the 0°C ammonia flow to $v_0 = 0.399$ m/s for $u_v = 10$ m/s *versus* $v_0 = 0.732$ m/s when $u_v = 20$ m/s. If the flow tem-

perature is taken into consideration, both the mass transfer coefficient and the mass flux are higher in lower temperature flows. It is worth noting that for the considered example flows, the model solution falls in the transition region where the general dependency between the parameters k^+ and τ^+ changes from square proportionality ($k^+ \sim \tau^{+2}$) to virtual independency of k^+ from τ^+ ($k^+ = \text{const}$ for $\tau^+ > 22.87$) [18]. These relations are depicted in Fig. 2 by dotted lines.

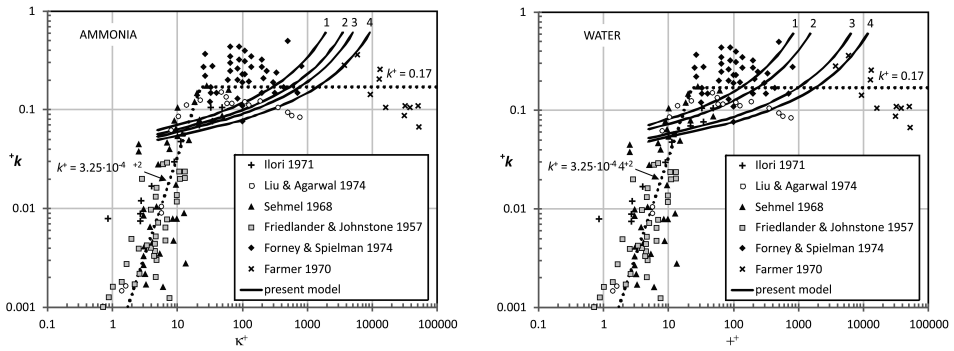

Figure 2: Solutions of separation equation (42) for ammonia (left) and water (right) vapour-droplet flows at saturation conditions in vertical pipe of 0.1 m ID compared to experimental results (scattered points). Four calculated curves are presented for each fluid. For ammonia, the flow temperature (T_ν), velocity of vapour (u_ν) and min./max. droplet diameters (D) were, respectively: 1) -30°C, 10 m/s, 6.4/125 μm; 2) -30°C, 20 m/s, 3.5/92 μm; 3) 0°C, 10 m/s, 4.6/146 μm; 4) 0°C, 20 m/s, 2.5/108 μm. For water flow these parameters were: 1) 100°C, 10 m/s, 9.4/122 μm; 2) 100°C, 20 m/s, 5.1/90 μm; 3) 200°C, 10 m/s, 4.7/168 μm; 4) 200°C, 20 m/s, 2.6/124 μm.

4 Summary

The simplified droplet (solid particle) separation theory presented in the paper returns satisfactory results. Analytical correlations obtained through the current research allow for determination of the influence of particular parameters on the complex process of a droplet (solid particle) separation. It is worth to emphasise that mentioned separation process depends on a statistical droplet distribution which is unsteady and it varies with the channel length due to larger drops separation before smaller ones. This effect is usually not being considered in the analytical studies. The paper mainly presents the inertia-diffusion mechanism of a droplet separation from the two-phase (vapour-liquid) flow. It was noted that droplets falling

in the area of the boundary layer rotate which directly results from the presence of the high velocity gradients. This causes a significant impact on the distance range at which droplets separate and deposit on the channel wall. The author's original droplet separation mechanism was developed based on inertia and turbulent diffusion. The developed droplet separation mechanisms allow for designing separator channels of varying geometries.

Received 14 May 2021

References

[1] Sedler B., Mikielewicz J.: *A simplified analytical flow-boiling crisis mode*. Trans. Inst. Fluid-Flow Mach. **76**(1978), 3–10 (in Polish).

[2] Walley P., Hutchinson P., Hewitt G.F.: *The calculation of critical heat flux in forced convection boiling*. In: Proc. 5th Int. Heat Transfer Conf., Vol. II, Tokyo 1974.

[3] Kubski P., Mikielewicz J.: *Approximated analysis of the drag force of the droplet evaporating within the fluid flow*. Trans. Inst. Fluid-Flow Mach. **81**(1981), 53–66 (in Polish).

[4] Mikielewicz J.: *A simplified analysis of Magnus lift force impact on a small droplets separation from the two-phase flow*. Trans. Inst. Fluid-Flow Mach. **75**(1978), 63–71 (in Polish).

[5] Ranhiainen P.O., Stachiewicz J.W.: *On the deposition of small particles from turbulent streams*. J. Heat Transfer. **92**(1970), 1, 169–177.

[6] Dolna O., Mikielewicz J.: *Separation of droplets in the field of a boundary layer*. J. Eng. Phys. Thermophys. **92**(2019), 5, 1202–1206.

[7] Pourhashem H., Owen M.P., Castro N.D., Rostami A.A.: *Eulerian modeling of aerosol transport and deposition in respiratory tract under thermodynamic equilibrium condition*. J. Aerosol Sci. **141**(2020), 105501.

[8] Worth Longest P., Xi J.: *Computational investigation of particle inertia effects on submicron aerosol deposition in the respiratory tract*. J. Aerosol Sci. **38**(2007), l, 111–130.

[9] Wang Y., Yu Y., Hu D., Xu D., Yi L., Zhang Y., Zhang S.: *Improvement of drainage structure and numerical investigation of droplets trajectories and separation efficiency for supersonic separators*. Chem. Eng. Process. – Process Intensific. **151**(2020), 107844.

[10] Ganic E.N., Rohsenow W.M.: *Dispersed flow heat transfer*. Int. J. Heat Mass Tran. **20**(1977), 8, 855-866.

[11] Beek W.J., Muttzal K.M.: *Transport Phenomena*. Wiley 1975.

[12] Hutchinson P., Hewitt G.F., Ducler A.E.: *Deposition of liquid or solid dispersions from turbulent gas stream: a stochastic model*. Chem. Eng. Sci. **26**(1971), 3, 419–439.

[13] Farmer R.A., Griffith P., Rohsenow W.M.: *Liquid droplet deposition in two-phase flow.* J. Heat Transfer **92**(1970), 4, 587–594.

[14] Forney L.J., Spielman L.A.: *Deposition of coarse aerosols from turbulent flow.* J. Aerosol Sci. **5**(1974), 3, 257–271.

[15] Friedlander S.K., Johnstone H.F.: *Deposition of suspended particles from turbulent gas streams.* Ind. Eng. Chem. **49**(1957), 7, 1151–1156.

[16] Ilori T.A.: *Turbulent deposition of particles inside pipes.* PhD thesis, Univ. Minnesota, Minneapolis – Saint Paul 1971.

[17] Sehmel G.A.: *Aerosol deposition from turbulent airstreams in vertical conduits.* Pacific Northwest Lab. Tech. Rep. BNWL-578, Richland 1968.

[18] McCoy D.D., Hanratty T.J.: *Rate of deposition of droplets in annular two-phase flow.* Int. J. Multiphas. Flow **3**(1977), 4, 319–331.